

## The composition of 433 Eros: A mineralogical–chemical synthesis

T. J. McCOY<sup>1</sup>, T. H. BURBINE<sup>1</sup>, L. A. McFADDEN<sup>2</sup>, R. D. STARR<sup>3</sup>, M. J. GAFFEY<sup>4†</sup>, L. R. NITTLER<sup>5‡</sup>,  
L. G. EVANS<sup>6</sup>, N. IZENBERG<sup>7</sup>, P. G. LUCEY<sup>8</sup>, J. I. TROMBKA<sup>5</sup>, J. F. BELL, III<sup>9</sup>, B. E. CLARK<sup>5</sup>, P. E.  
CLARK<sup>3</sup>, S. W. SQUYRES<sup>9</sup>, C. R. CHAPMAN<sup>10</sup>, W. V. BOYNTON<sup>11</sup> AND J. VEVERKA<sup>9</sup>

<sup>1</sup>Department of Mineral Sciences, National Museum of Natural History, Smithsonian Institution, Washington, D.C. 20560-0119, USA

<sup>2</sup>Department of Astronomy, University of Maryland, College Park, Maryland 20742, USA

<sup>3</sup>Physics Department, The Catholic University of America, Washington, D.C. 20064, USA

<sup>4</sup>Department of Earth and Environmental Sciences, Rensselaer Polytechnic Institute, Troy, New York 12180, USA

<sup>5</sup>Laboratory for Extraterrestrial Physics, Code 691, NASA Goddard Space Flight Center, Greenbelt, Maryland 20771, USA

<sup>6</sup>Science Programs, Computer Sciences Corporation, Laurel, Maryland 20706, USA

<sup>7</sup>Johns Hopkins University Applied Physics Laboratory, 11100 Johns Hopkins Road, Laurel, Maryland 20723, USA

<sup>8</sup>Hawaii Institute of Geophysics and Planetology, University of Hawaii, Honolulu, Hawaii 96822, USA

<sup>9</sup>Department of Astronomy, Space Sciences Building, Cornell University, Ithaca, New York 14853, USA

<sup>10</sup>Southwest Research Institute, 1050 Walnut Street, Suite 426, Boulder, Colorado 80302, USA

<sup>11</sup>Lunar and Planetary Laboratory, University of Arizona, Tucson, Arizona 85721, USA

†Present address: Department of Space Studies, University of North Dakota, Grand Forks, North Dakota 58202-9008, USA

‡Present address: Department of Terrestrial Magnetism, Carnegie Institution of Washington, 5241 Broad Branch Road Northwest, Washington, D.C. 20015, USA

\*Correspondence author's e-mail address: [mccoy.tim@nmnh.si.edu](mailto:mccoy.tim@nmnh.si.edu)

(Received 2001 August 1; accepted in revised form 2001 August 24)  
(Part of a series of papers on the NEAR–Shoemaker mission to 433 Eros)

**Abstract**—The near-Earth asteroid rendezvous (NEAR) mission carried x-ray/gamma-ray spectrometers and multi-spectral imager/near-infrared spectrometer instrument packages which gave complementary information on the chemistry and mineralogy, respectively, of the target asteroid 433 Eros. Synthesis of these two data sets provides information not available from either alone, including the abundance of non-mafic silicates, metal and sulfide minerals. We have utilized four techniques to synthesize these data sets. Venn diagrams, which examine overlapping features in two data sets, suggest that the best match for 433 Eros is an ordinary chondrite, altered at the surface of the asteroid, or perhaps a primitive achondrite derived from material mineralogically similar to these chondrites. Normalized element distributions preclude FeO-rich pyroxenes and suggest that the x-ray and gamma-ray data can be reconciled with a common silicate mineralogy by inclusion of varying amounts of metal. Normative mineralogy cannot be applied to these data sets owing to uncertainties in oxygen abundance and lack of any constraints on the abundance of sodium. Matrix inversion for simultaneous solution of mineral abundances yields reasonable results for the x-ray-derived bulk composition, but seems to confirm the inconsistency between mineral compositions and orthopyroxene/clinopyroxene ratios. A unique solution does not seem possible in synthesizing these multiple data sets. Future missions including a lander to fully characterize regolith distribution and sample return would resolve the types of problems faced in synthesizing the NEAR data.

### INTRODUCTION

The near-Earth asteroid rendezvous (NEAR)–Shoemaker mission spent almost a year in orbit around the asteroid 433 Eros, studying its mineralogy, surface chemistry, surface geology, surface topography, and gravitational and magnetic fields. This is the first time that such a diverse suite of data has been collected simultaneously from an asteroid by a spacecraft. 433 Eros is a particularly worthy target for this study, since

ground-based spectral studies (Murchie and Pieters, 1996) indicate that it is a member of the S(IV) spectral class of Gaffey *et al.* (1993). Debate has raged for nearly 20 years about the relationship between S asteroids and ordinary chondrites (Wetherill and Chapman, 1988), the most abundant types of asteroids in the inner belt and meteorites observed to fall to Earth, respectively, and NEAR may allow solution of this conundrum, if only in this one specific case. While each data set can be interpreted individually, as evidenced by the series of papers

presented in this special issue of *Meteoritics and Planetary Science*, the real strength of the NEAR mission is the ability to synthesize multiple data sets to address a common problem.

In this paper, we synthesize the mineralogy and chemical composition determined by independent analyses of spectra from the near-infrared spectrometer (NIS) and multi-spectral imager (MSI) and the x-ray and gamma-ray spectrometers (XGRS), respectively. Details of these instruments and results from these experiments are given elsewhere and only brief review is necessary here. The NIS (Warren *et al.*, 1997; Peacock *et al.*, 1998) acquired 0.8–2.6  $\mu\text{m}$  reflectance spectra and the multi-spectral imager (Hawkins *et al.*, 1997; Hawkins, 1998) mapped the surface using seven narrow band filters from 0.45 to 1.05  $\mu\text{m}$ . Reflectance spectra can be used to determine the type and abundance of FeO-bearing mafic silicates, notably olivine and pyroxene. The x-ray spectrometer (Goldsten *et al.*, 1997; Trombka *et al.*, 1997; Goldsten, 1998) measured discrete x-ray emissions of Mg, Si, Al, S, Ca and Fe from the upper 100  $\mu\text{m}$  of the surface. The gamma-ray spectrometer measured gamma-ray emission from Fe, Mg, Si, O and K in the upper tens of centimeters, generated by cosmic rays and natural radioactivity while on the surface of the asteroid.

Data from the MSI/NIS and XGRS instruments can be compared with chemical, mineralogical and spectral data from meteorites, potentially allowing us to link 433 Eros to a known meteorite type. Further, we can infer the geologic processes that may have formed or altered 433 Eros by comparison to the processes that formed the analog meteorites. However, much of the chemical and mineralogical data known for meteorites is not measured by either the MSI/NIS or XGRS instruments, but must be inferred from a synthesis of these two data sets. This includes the complete suite of minerals present (including non-mafic silicates, metal and sulfide), the composition of the minerals (particularly olivine and pyroxene compositions) and the partitioning of iron between silicates, metal and sulfide. These parameters are widely used in meteorite classification and their determination is essential in comparing Eros to meteorite types.

In this paper, we report our efforts to synthesize chemical and mineralogical data sets to investigate (1) the relationship between 433 Eros and known meteorite types using the available constraints from these two instrument packages and (2) the mineralogy, mineral abundances and mineral compositions of 433 Eros.

## DATA AND CONSTRAINTS

Mineralogical and chemical constraints on the composition of 433 Eros are given and discussed elsewhere (Lucey *et al.*, 2001; McFadden *et al.*, 2001; Nittler *et al.*, 2001; Evans *et al.*, 2001) and we briefly review only the major constraints for synthesizing these multiple data sets here. Table 1 lists the chemical composition interpreted from the x-ray and gamma-ray experiments and the mineralogy and mineral compositions interpreted from the MSI/NIS experiments.

TABLE 1. Mineralogical–chemical constraints from XGRS and MSI/NIS data sets.

Element/ element ratio	XRS	GRS
<b>Chemical Constraints</b>		
Mg/Si	$0.85 \pm 0.11$	0.75
Fe/Si	$1.65 \pm 0.27$	0.8
Al/Si	$0.068 \pm 0.022$	–
S/Si	$0.014 \pm 0.017$	–
Ca/Si	$0.077 \pm 0.006$	–
Si/O	–	0.53–0.67
Fe/O	–	0.16–0.44
K	–	0.07 wt%
<b>Mineralogical Constraints</b>		
"Thermospectra" ( $\Delta\text{Reflectance}/\Delta T$ vs. Wavelength)		
Eros = "Olivine-rich" (e.g., LL, CO)		
Eros $\neq$ "Pyroxene-rich" (e.g., H)		
Band Positions and Band Area Ratios		
One-pyroxene model		
Opx/(opx + ol) = 0.42		
Composition of $\text{Fs}_{40-65}\text{Wo}_{10-20}$		
Two-pyroxene model		
76% $\text{Fs}_{15}\text{Wo}_{<11}$ 24% $\text{Fs}_{10}\text{Wo}_{45}$		
83% $\text{Fs}_{25}\text{Wo}_{<11}$ 17% $\text{Fs}_{10}\text{Wo}_{45}$		

The chemical composition of the surface of 433 Eros is discussed at length by Nittler *et al.* (2001). These authors derived the composition of Eros using x-ray spectroscopy during the period of five solar flares, each covering a spot of a few square kilometers, and two periods of "quiet Sun", which are essentially hemispheric measurements. They argue that no significant compositional variability is present on the surface of Eros and, thus, they calculate a global average composition for Eros. Average values for Mg/Si, Fe/Si, Al/Si and Ca/Si are given in Table 1, along with the  $1\sigma$  standard deviation of the individual analyses. Nittler *et al.* (2001) argue that the standard error of the mean, which in each case is less than the  $1\sigma$  standard deviation, is a better measure of the true uncertainty in the average composition. However, we use the more conservative estimates of uncertainty (the  $1\sigma$  standard deviation) for this study. Nittler *et al.* (2001) argue that the S/Si ratio is best expressed as an upper limit of 0.05. We use the average S/Si ratio of  $0.014 \pm 0.017$  reported by these authors, since many of our integrative techniques are numerical and require absolute values, rather than upper limits.

Although NEAR carried a gamma-ray spectrometer, orbital measurements of the composition of 433 Eros were hampered by low signal/noise ratios. Evans *et al.* (2001) discuss this problem at length and report *in situ* compositions taken with the gamma-ray spectrometer after a controlled descent to the surface of Eros. It is important to note that these measurements were probably taken in an unrepresentative spot on the asteroid

(the edge of a pond deposit; Veverka *et al.*, 2001) and that the gamma-ray-derived composition is from greater depth (tens of centimeters) than the x-ray-derived composition (tens of microns). The gamma-ray-derived composition has an essentially chondritic Mg/Si ratio (overlapping the x-ray-derived Mg/Si ratio) and K abundance, but Fe/O and Fe/Si are significantly depleted relative to ordinary chondrites. This composition is best interpreted (Evans *et al.*, 2001) as separation of metal-sulfide from silicates by physical migration in the thick regolith on 433 Eros.

The combined data sets of the MSI and NIS measured the spectrum of the 433 Eros from 816 to 2363 nm covering both the 1  $\mu\text{m}$  spectral absorption feature (due to FeO-bearing olivine and pyroxene) and the 2  $\mu\text{m}$  absorption feature (due to FeO-bearing pyroxene only) (McFadden *et al.*, 2001). A remarkable feature of 433 Eros is its virtual lack of any spectral heterogeneity. The spectra of 433 Eros (Veverka *et al.*, 2000) are unlike laboratory-based spectra of known meteorites (Clark *et al.*, 2001) and, thus, direct spectral comparison between Eros and laboratory reflectance spectra of possible meteoritic analogs yields a negative result. A variety of other techniques have been used. Lucey *et al.* (2001) modelled "thermospectra"—the change in reflectance with change in temperature over each wavelength—to argue that 433 Eros is "olivine-rich". They argue that while LL and CO chondrites would satisfy such a criteria, H chondrites would not, although they cannot readily quantify the modal abundances or mineral compositions from this technique. Clark *et al.* (2001) fit the entire spectrum of Eros using a model with five mineral end members and derived olivine/orthopyroxene ratios of 75:25, slightly greater than observed in LL chondrites (see Table 2), and slightly higher than the ratio (58:42) derived from band area analyses of NIS data (McFadden *et al.*, 2001).

The most widely used technique for estimating mineralogy and mineral composition from remotely-sensed spectral data is using band parameters. Specifically, the band I center is a function of both pyroxene composition and olivine/pyroxene ratio, the band II center is a function of the pyroxene composition, and the band area ratio (band II area/band I area) is a function of the olivine/pyroxene ratio (Cloutis *et al.*, 1986). McFadden *et al.* (2001) have derived these values for 433 Eros. The data can be interpreted in two different ways. If 433 Eros contains only a single pyroxene, McFadden *et al.* (2001) derive a composition for a single pyroxene of Fs<sub>58–65</sub> and Wo<sub>11–13</sub> with an olivine/orthopyroxene ratio of 58:42 (similar to H chondrites). Gaffey (pers. comm.) derives a somewhat lower FeO concentration (Fs<sub>40–50</sub>) and broader range of possible calcium concentrations (Wo<sub>10–20</sub>). These authors consider these FeO-rich pyroxene compositions (Fs<sub>40–65</sub>) unlikely, given that it is outside the range of chondrites for Wo and above the range for ordinary chondrites for Fs.

A more likely scenario is that Eros, by analogy with chondritic meteorites, contains two pyroxenes—a dominant orthopyroxene and a subordinate calcic pyroxene. McFadden

*et al.* (2001) explore such a scenario. To satisfy the spectral parameters, a tradeoff exists between the abundance of clinopyroxene and the FeO concentration in orthopyroxene. One can thus constrain these relative abundances of ortho- and clinopyroxene and the composition of orthopyroxene to a range that satisfies the band area parameters. If we bracket likely ranges using pyroxene compositions of Fs<sub>15–25</sub> (comparable to the range for ordinary chondrites), we find corresponding clinopyroxene abundances of 24% to 17%, respectively. McFadden *et al.* (2001) argue that this range of compositions best overlaps the observed mineral compositions and normative abundances for LL chondrites, although they are clearly close to L chondrites. H chondrites require an overabundance of calcic pyroxene relative to calculated normative values (McSween *et al.*, 1991) or an uncertainty in the band parameters ( $\pm 0.05 \mu\text{m}$ ) which is seemingly too large. Alternatively, one might satisfy the band parameters by increasing the calcic pyroxene abundance through injection of a basaltic partial melt, such as is observed in some primitive achondrites (McCoy *et al.*, 2000).

## RESULTS

We have considered four approaches to synthesizing these NEAR data sets: (1) Venn diagrams, (2) normalized elemental distributions, (3) normative mineralogy, and (4) matrix inversion. We discuss each of these in turn, focusing on the results of the analyses and implications for the compositions of 433 Eros and its relationship to known groups of meteorites.

### Venn Diagrams

Venn diagrams provide a useful tool for comparing the properties of two sets of information and determining areas of overlap. In this case, we populate our Venn diagram (Fig. 1) with groups of meteorites permissible as analogs for Eros on the basis of, respectively, the MSI/NIS and XGRS data sets.

Both data sets exclude a wide range of meteorite types. Although both lunar and Martian meteorites could be excluded *a priori*, their compositions and mineralogies are poor matches for 433 Eros. Aubrites, EH and EL chondrites fall outside the compositional ranges of both the x-ray and gamma-ray compositions for Mg/Si, Ca/Si and Fe/O (Nittler *et al.*, 2001; Evans *et al.*, 2001). More importantly, such highly-reduced meteorite groups have essentially FeO-free silicates (Keil, 1989) and, thus, would not exhibit the 1 and 2  $\mu\text{m}$  spectral absorption features typical of FeO-bearing silicates and present in spectra of Eros (Veverka *et al.*, 2000).

The howardite–eucrite–diogenite (HEDs) suite of meteorites are products of partial melting, fractional crystallization and impact mixing. Eucrites are markedly enriched in Al/Si relative to the composition of 433 Eros and all three groups are depleted in Mg/Si relative to the x-ray derived value, although similarities do exist between these groups and the gamma-ray derived Fe/Si,

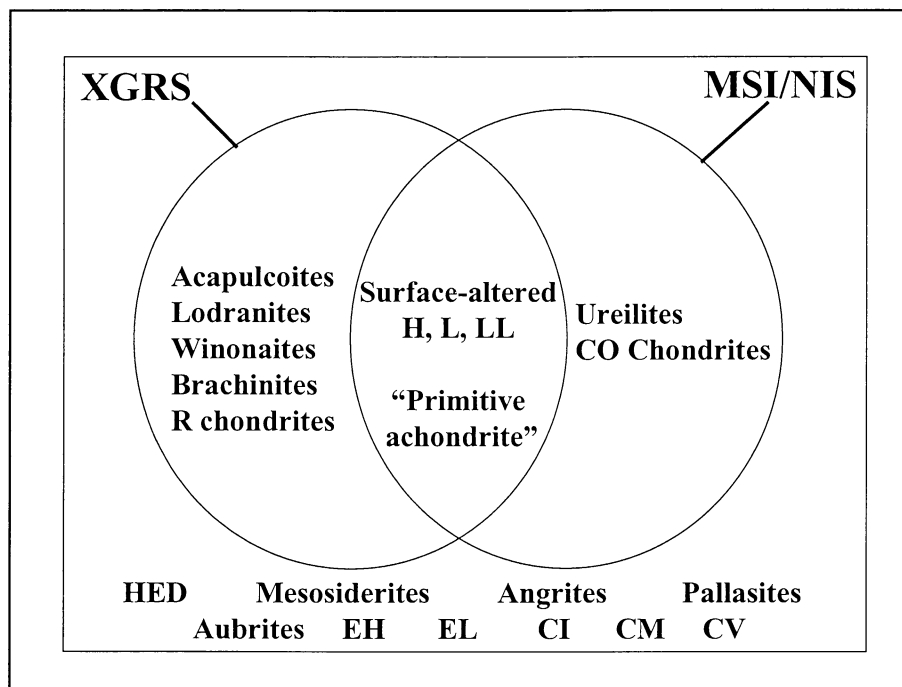


FIG. 1. Venn diagram for the XGRS and MSI/NIS data sets. Those meteorites included in the box but outside the circles are prohibited by both data sets. Those in a circle but outside the intersection are allowed by one data set but not the other. The most likely meteoritic analogs to 433 Eros appear to be H, L, LL or CO chondrites which have been altered at the surface of the asteroid or a type of primitive achondrite derived from a precursor with a mineralogy similar to these chondrites.

Si/O and Fe/O ratios (Nittler *et al.*, 2001). Further, their spectra and band parameters differ substantially from Eros. The strength of the  $2\ \mu\text{m}$  band relative to the  $1\ \mu\text{m}$  band is much greater in HED group, reflecting their pyroxene-rich nature. The same is true of mesosiderites, which are basaltic-pyroxenitic fragments mixed with metal. Likewise, the basaltic Angrites, which are dominated by Ti-augite, tend to exhibit no  $2\ \mu\text{m}$  feature (Burbine *et al.*, 2001a) and have substantially higher Al/Si and Ca/Si ratios than Eros (Nittler *et al.*, 2001). The pallasites, in contrast, are substantially depleted in Al/Si relative to Eros and have no  $2\ \mu\text{m}$  feature.

CI and CM chondrites are reasonable matches for the x-ray-derived Mg/Si and Fe/Si ratios, but poor matches for x-ray-derived Al/Si or Ca/Si or any of the gamma-ray-derived composition. They can be further excluded based on the absence of a water of hydration band in the Eros spectrum (Eaton *et al.*, 1983) (which would be expected of either CI or CM) and the greater density of Eros compared to CI chondrites. CV chondrites have comparable Fe/Si and Mg/Si ratios to the x-ray-derived values for Eros, but higher Al/Si and Ca/Si. Their spectral band area ratios (derived from Gaffey, 1976) imply higher olivine/pyroxene ratios than for Eros and, although bulk modal analyses are not known, certain members (*e.g.*, Allende; Clarke *et al.*, 1970) are known to be quite olivine-rich.

Several groups of meteorites are consistent with the x-ray data, but inconsistent with the MSI/NIS constraints. R chondrites have Mg/Si, Fe/Si and Al/Si ratios within the range of the x-ray

data. However, band center and area parameters derived from laboratory-based spectra of the R-chondrite Rumuruti (Burbine and McCoy, unpubl. data) are inconsistent with those for Eros. Rumuruti has a band area ratio consistent with a nearly-pure olivine assemblage. Among the groups of primitive achondrites—meteorites that have experienced limited degrees of partial melting and melt migration—the acapulcoites, lodranites, brachinites and winonaites all have bulk chemical compositions which are broadly consistent with the x-ray and gamma-ray derived composition for 433 Eros (Nittler *et al.*, 2001). However, the mineral assemblages inferred from the spectral band parameters are inconsistent with a link between 433 Eros and these meteorites (Burbine *et al.*, 2001b). Acapulcoites, lodranites and winonaites all appear to have more pyroxene-rich compositions than derived for Eros, although individual members of these groups, particularly the lodranites, may match Eros. Further, the spectral heterogeneity one might expect from the parent bodies of these groups (McCoy *et al.*, 2000) is not observed on Eros. In contrast to these other groups, brachinites are dominated by olivine and pyroxene features are essentially absent in their spectra. This is in sharp contrast to Eros, which has pyroxene spectral absorption bands and, thus, Eros is not parental to the brachinites.

In contrast, ureilites have ol/(ol + opx) ratios consistent with those derived from band area parameters (Mittlefehldt *et al.*, 1998), but the albedo of Eros is higher and chemical compositions, particularly for Mg/Si and Al/Si are inconsistent

with values derived by the x-ray spectrometer. CO chondrites have thermospectra (Lucey *et al.*, 2001) and, at least for some members of the CO group, band area ratios similar to Eros. The Fe/Si and Mg/Si ratios are also close to Eros. However, the Al/Si and Ca/Si ratios for Eros would seem to preclude CO chondrites, which tend to have higher Al and Ca abundances relative to Si (Nittler *et al.*, 2001). We include ureilites and CO chondrites in the MSI/NIS portion of our Venn diagram on the basis of their ol/(ol + px) ratios, although we recognize the albedo differences.

While it is probably impossible to identify a unique link between a single group of meteorites and 433 Eros, several kinds of meteorites are reasonable candidates. The x-ray-derived Fe/Si ratio for 433 Eros is most consistent with H chondrites, although  $2\sigma$  uncertainties would allow L and LL chondrites as well. The Al/Si, Mg/Si and Ca/Si ratios are relatively invariant between H, L and LL chondrites. The x-ray-derived S/Si ratio is about one-half that of ordinary chondrites (Nittler *et al.*, 2001). Further, the gamma-ray derived Fe/O ratio is about one-half that of ordinary chondrites (Evans *et al.*, 2001). The only geologic explanation consistent with both sets of data is that alteration through impact volatilization, sputtering and physical segregation of metal and sulfide in the regolith produced the observed compositions (Nittler *et al.*, 2001; Evans *et al.*, 2001). Distinguishing whether the bedrock is H, L or LL is probably not possible from these altered compositions, and spectral data do not point to a unique solution. Thermospectra (Lucey *et al.*, 2001) point to an L or LL chondritic asteroid, while derived olivine/pyroxene ratios are consistent with H, L or LL chondrites, depending on the method of analysis (Clark *et al.*, 2001; McFadden *et al.*, 2001). Thus, while an ordinary chondritic composition for 433 Eros is a likely possibility, deciding between the chemical groups appears difficult if not impossible, particularly in light of the inferred mobility of S and Fe.

Since there is no evidence that we have a sample of 433 Eros in our collections, one might reasonably ask whether another type of rock not known as a meteorite might satisfy the mineralogical and chemical constraints. The answer is perhaps. Metal and sulfide melting and melt migration might equally well explain the difference between the XRS and GRS compositions. Low degree partial melting is a hallmark of the primitive achondrites. While known groups of primitive achondrites are inconsistent with the data, we can envision that asteroids with essentially ordinary chondrite mineral abundances underwent limited partial melting on a localized scale, producing a type of primitive achondrite not sampled in our collections. One problem with this theory is the relative homogeneity of 433 Eros, which, as noted earlier, is difficult to reconcile with a primitive achondritic body, irrespective of the composition of that body.

Based on this Venn diagram approach, we suggest that the bedrock of 433 Eros is most likely an ordinary chondrite (H, L, LL) or a type of primitive achondrite not sampled on Earth (partially-melted but with an olivine/pyroxene ratio similar to

ordinary chondrites. The near-surface composition has almost certainly been altered by a variety of processes.

### Normalized Elemental Distribution

The second method we have applied is an attempt to calculate the mineralogy using elemental ratios. This technique has several advantages. First, it utilizes elemental ratios, allowing us to avoid complex geometric effects attendant with deriving absolute elemental abundances from x-ray and gamma-ray remote-sensing spectra. Secondly, it allows us to allocate Fe between primary Fe-bearing phases using the relationship:

$$Fe_{\text{metal}}/Si = Fe_{\text{total}}/Si - Fe_{\text{silicate}}/Si - Fe_{\text{sulfide}}/Si$$

where  $Fe_{\text{total}}/Si$  is the x-ray or gamma-ray derived values from NEAR. The  $Fe_{\text{sulfide}}/Si$  is constrained by the measured S/Si ratio and the Fe/S ratio for troilite (FeS). The  $Fe_{\text{silicate}}/Si$  ratio is determined from the inferred mafic silicate compositions (fayalite in olivine, ferrosilite in pyroxene) and the measured Mg/Si ratio (constraining the mafic silicate abundance). The Al/Si and Ca/Si ratios constrain plagioclase abundance. An example of the detailed mathematical treatment for this method is given in Appendix A and a summary of results with a range of variables is given in Table 2.

It is worth discussing both the assumptions and constrained variables necessary to apply this method. The  $Fe_{\text{silicate}}/Si$  ratio ultimately depends on the compositions of olivine and pyroxene(s), their relative abundances and the Mg/Si compositional ratio for 433 Eros. As discussed earlier, several of these parameters are constrained by x-ray, gamma-ray, visible and near-infrared spectrometry for 433 Eros. For these calculations, we used orthopyroxene compositions of ferrosilite 15, 25 and 40 (with correspondingly constrained orthopyroxene/clinopyroxene ratios) and olivine/pyroxene ratios (75:25 and 58:42) given by Clark *et al.* (2001) and McFadden *et al.* (2001). Mg/Si ranged between 0.75 and 0.85, the derived gamma-ray and x-ray measurements, respectively. Olivine composition was constrained using a ratio of Fa/Fs of 1.18, appropriate to solid-state partitioning of Fe between co-existing olivines and pyroxenes in ordinary chondrites measured by Gomes and Keil (1980).

The  $Fe_{\text{sulfide}}/Si$  ratio depends on the assumed Fe/S ratio. We assumed an atomic ratio of 1, appropriate to stoichiometric troilite (FeS), which is the dominant sulfide phase in most moderately-oxidized meteorites. The plagioclase abundances depends on an assumed Al/Si ratio for plagioclase, which we took as a value appropriate to an ordinary chondrite composition of  $An_{12.6}Or_{3.6}$ . The  $Fe_{\text{metal}}/Si$  ratio is obviously sensitive to the observed Fe/Si ratio for 433 Eros. We let Fe/Si for 433 Eros range between 0.8 (the gamma-ray determination) and 1.65 (the global average for the x-ray determination).

With a moderately-complicated mathematic treatment such as this, error propagation becomes non-trivial. We approach

the problem of error propagation by calculating a matrix of possible solutions using a range of variables (Table 2). The results of these calculations provide some indications of the range of compatible mineralogical and chemical variables. Compositions calculated using the one-pyroxene model of McFadden *et al.* (2001) are difficult to reconcile with the x-ray and gamma-ray chemical compositions. We used a composition of Fs<sub>40</sub>, which is at the low end of allowable orthopyroxene compositions in the one-pyroxene model. When combined with the average Mg/Si (0.85) and Fe/Si (1.65) ratios from the x-ray experiment (column 1), an overabundance of mafic silicate (>100%) is indicated. If we use the gamma-ray derived Mg/Si ratio (0.75) (column 2), we can produce a mineralogy with constrained olivine and pyroxene abundances of 55 and 40 wt%, respectively. The metal abundance (5.0 wt%) is relatively low and troilite is <1 wt%, as expected from the low S/Si ratio. Thus, we conclude that it is possible to reconcile x-ray Fe/Si ratio with the FeO-rich pyroxene composition of the one-pyroxene model. However, it is reasonable to ask whether the same mineral compositions (a reasonable assumption for a body of chondritic or near-chondritic composition) are consistent with the much lower Fe/Si ratio derived by the gamma-ray spectrometer (column 3). As Table 2 illustrates, they cannot be reconciled. The FeO-rich orthopyroxene composition of the one-pyroxene model would require negative abundances of metal (-19.2 wt%)—clearly an unreasonable solution. Our calculations support the contention of McFadden *et al.* (2001) that such an FeO-rich pyroxene composition is unreasonable.

We consider the two-pyroxene model of McFadden *et al.* (2001) by calculating a range of mineralogies using compositions constrained by both Fs<sub>15</sub> and Fs<sub>25</sub> orthopyroxene compositions. A few trends are worth noting. Changing the olivine/pyroxene ratio and the pyroxene composition have unexpected consequences. A change in olivine/pyroxene ratio from 75:25 to 58:42 results in an 8–10% increase in (ol + px) abundance (*e.g.*, columns 4 vs. 6) and a change in pyroxene composition from Fs<sub>25</sub> to Fs<sub>15</sub> at a constant olivine/pyroxene ratio of 58:42 (*e.g.*, columns 6 vs. 9) results in an ~5% decrease in (ol + px) abundance. These changes reflect the dependence of mafic silicate abundance on Mg/Si ratio, which differs markedly between olivine and pyroxene and between pyroxenes of different composition. Metal abundances are relatively insensitive to olivine/pyroxene ratio (*e.g.*, columns 5 vs. 8), but metal abundance increases by ~5 wt% with a change from Fs<sub>25</sub> to Fs<sub>15</sub> (*e.g.*, columns 6 vs. 9). Plagioclase is somewhat overabundant at all compositions relative to ordinary chondrites (~10 wt%). As expected, troilite comprises <1% of each calculated mineralogy.

Applying the same test used for the Fs<sub>40</sub> orthopyroxene composition in the one-pyroxene case, we ask whether we can reconcile both the x-ray and gamma-ray compositions with a single mineral composition. The simple answer is yes. If we calculate a mineralogy with a orthopyroxene of Fs<sub>25</sub> and the global average x-ray composition for Mg/Si and Fe/Si (column 6), we can find a mineralogy of 44% olivine, 26%

TABLE 2. Derived mineralogies using the normalized element distribution technique and a range of olivine/pyroxene ratios, orthopyroxene compositions, and Mg/Si and Fe/Si ratios.

Property	Source	1	2	3	4	5	6	7	8	9	10	H\$	L\$	LL\$
OI/Px	MSI/NIS*	58:42	58:42	58:42	75:25	75:25	58:42	58:42	58:42	58:42	58:42	54:46	61:39	66:34
Opx/Cpx	MSI/NIS†	100:0	100:0	100:0	83:17	83:17	83:17	83:17	83:17	76:24	76:24	86:14	83:17	80:20
Opx Comp.	MSI/NIS†	Fs <sub>40</sub> Wo <sub>0</sub>	Fs <sub>40</sub> Wo <sub>0</sub>	Fs <sub>40</sub> Wo <sub>0</sub>	Fs <sub>25</sub> Wo <sub>0</sub>	Fs <sub>25</sub> Wo <sub>0</sub>	Fs <sub>25</sub> Wo <sub>0</sub>	Fs <sub>25</sub> Wo <sub>0</sub>	Fs <sub>25</sub> Wo <sub>0</sub>	Fs <sub>15</sub> Wo <sub>0</sub>	Fs <sub>15</sub> Wo <sub>0</sub>	Fs <sub>17.2</sub>	Fs <sub>21.3</sub>	Fs <sub>24.1</sub>
Ol Comp.	Assumed‡	Fa <sub>47</sub>	Fa <sub>47</sub>	Fa <sub>47</sub>	Fa <sub>30</sub>	Fa <sub>30</sub>	Fa <sub>30</sub>	Fa <sub>30</sub>	Fa <sub>30</sub>	Fa <sub>18</sub>	Fa <sub>18</sub>	Fa <sub>18.8</sub>	Fa <sub>24.6</sub>	Fa <sub>28.5</sub>
Cpx Comp.	Assumed§	N/A	N/A	N/A	Fs <sub>10</sub> Wo <sub>45</sub>	Fs <sub>10</sub> Wo <sub>45</sub>	Fs <sub>10</sub> Wo <sub>45</sub>	Fs <sub>10</sub> Wo <sub>45</sub>	Fs <sub>10</sub> Wo <sub>45</sub>	Fs <sub>10</sub> Wo <sub>45</sub>	Fs <sub>10</sub> Wo <sub>45</sub>	—	—	—
Mg/Si	XRS-GRS#	0.85	0.75	0.75	0.85	0.75	0.75	0.75	0.75	0.85	0.75	0.8	0.8	0.8
Fe/Si	XRS-GRS#	1.65	1.65	0.8	1.65	0.8	1.38	0.8	0.8	1.65	0.8	1.0	1.2	1.6
Olivine	Calculated	64.7	54.6	68.4	51.8	53	43.9	40.7	46	36	37.3	35.0	44.8	51.9
Opx	Calculated	46.9	39.5	49.6	14.3	14.7	26.4	24.5	27.6	19.8	20.5	26.2	24.2	21.4
Cpx	Calculated	0	0	0	2.9	3	5.4	5	5.7	6.2	6.5	4.1	5	5.3
Plag	Calculated	17.7	16.9	21.2	15.2	17.7	14.9	15.6	17.6	14	16.5	9.6	10.3	10.3
Metal	Calculated	0.5	5	-19.2	14.6	1	16.7	12.5	1.4	21.4	7.7	18.0	8.4	3.6
Sulfide	Calculated	1.1	0.9	1.1	0.7	0.7	0.8	0.7	0.8	0.7	0.7	5.5	5.8	5.9
Total	Calculated	130.9	116.9	121.1	99.5	90.1	108.1	99.0	99.1	98.1	89.2	98.4	98.5	98.4

\*Olivine/pyroxene ratios derived by Clark *et al.* (2001) and McFadden *et al.* (2001).

†Internally-consistent orthopyroxene/clinopyroxene ratios, orthopyroxene and clinopyroxene compositions using the one- and two-pyroxene models of McFadden *et al.* (2001).

‡Assumed using a Fa/Fs ratio of 1.18 appropriate to equilibrated ordinary chondrites (Gomes and Keil, 1980).

§Assumed average composition of clinopyroxene in ordinary chondrites (McFadden *et al.*, 2001).

#Values derived from the XRS and GRS measurements, including 1σ standard deviations (Nittler *et al.*, 2001; Evans *et al.*, 2001).

\$Average normative mineralogies (McSween *et al.*, 1991) and mineral compositions (Gomes and Keil, 1980) for H, L and LL chondrites.

orthopyroxene, 5% clinopyroxene, 14% plagioclase, 17% metal and 1% troilite. While this mineral composition is appropriate to L chondrites, the constrained olivine/pyroxene ratio (58:42) is more typical of H chondrites and the metal abundance is considerably greater than LL chondrites. Using the  $1\sigma$  lower limits of the global averages (column 7) produces ~12% metal, still greater than observed in LL chondrites. Nonetheless, it is possible to produce a mineral assemblage which satisfies both the mineral composition and chemical composition constraints. If we apply the gamma-ray derived composition (column 8), we can produce a mineralogy which satisfies these same constraints with only a trace (1 wt%) of metal. In short, both the x-ray and gamma-ray derived compositions can be explained by a mineral mixture constrained by an orthopyroxene composition of  $Fs_{25}$  with variable amounts of metal.

Finally, we reproduced these calculations with a  $Fs_{15}$  composition (columns 9 and 10). Interestingly, the same basic conclusions reached for the  $Fs_{25}$  composition apply. In this case, the  $Fs_{15}$  composition and olivine/pyroxene ratio are typical of H chondrites, while the orthopyroxene/clinopyroxene ratio is lower than observed in H chondrites and the metal ranges from slightly overabundant for the x-ray composition to heavily depleted for the gamma-ray composition. Thus, while we cannot decide between the  $Fs_{15}$  and  $Fs_{25}$  compositions, with both exhibiting some inconsistencies, we suggest that the x-ray and gamma-ray compositions can be reconciled with a common silicate mineralogy and mineral composition simply by varying the metal abundance, as also suggested by Evans *et al.* (2001).

### Normative Mineralogy

A normative mineralogy is calculated from the bulk chemical composition of a rock by partitioning oxides between minerals using a set of rules. A brief history of normative mineralogy calculations and the methods for calculating them is given by Cox *et al.* (1979). It is a conceptually simple method and has been used to determine mineral abundances for meteorites of known chemical composition (McSween *et al.*, 1991), as well as for rocks from the Mars Pathfinder mission (McSween *et al.*, 1999). Recent work by Gastineau and McSween (2000) suggest that the olivine/pyroxene ratio for meteorites derived from modal analysis is consistently lower than that from normative calculations, largely because of the presence of an  $SiO_2$ -rich glass shown to co-exist with olivine and pyroxene and not accounted for in the norm. In terrestrial rocks, it provides a means of comparing crystalline and glassy rocks, as well as determining the composition relative to the silica-saturation surface. In meteorites, the primary use has been to calculate the  $ol/(ol + px)$  ratio for comparison to remotely-sensed data from asteroids.

We have applied normative calculations to x-ray and gamma-ray data from Eros. Normative calculations assume a fixed FeO/MgO ratio in both olivine and pyroxene equivalent to the FeO/MgO ratio in the bulk rock. As such, independent

determination of the mineral compositions, such as those from MSI/NIS, are not needed for this calculation, although the consistency between the normative-derived values and the MSI/NIS-derived values can serve as a test of the method. We find several shortcomings with this technique that make it unsuitable for determining the mineralogy of 433 Eros. First, it requires absolute abundances of the oxides, rather than elemental ratios. One solution to this problem is to assume one elemental abundance and calculate the abundance of the remaining elements using the elemental ratios. Aluminum is relatively invariant between H, L and LL chondrites, with a concentration of ~1.2 wt%. We adopted this value as our assumed elemental abundance. From this value, we calculated values for Si, Ca, Fe, Mg, S and O.

The second problem with normative calculations is that they require knowledge of the partitioning of iron between silicates, metal and sulfides. Here, the metallic Fe abundance is determined by difference. Fe is combined first with S to form FeS. Oxygen is then combined with cations other than iron (Mg, Si, Ca, Al, K) and remaining O is combined with Fe to form FeO. Residual Fe is expressed as metallic iron. However, this technique requires uncertainties in the oxygen abundance to be smaller than the abundance differences that differentiate the groups of meteorites of interest. The oxygen abundance differs by ~10% relative between H and L chondrites and, thus, uncertainties better than ~5% relative are probably necessary to meaningfully determine the normative mineralogy. Stated uncertainties in the Fe/O ratio alone (Table 1) result in uncertainties in oxygen abundances of approximately a factor of 2 and full error propagation on the uncertainty of all elemental ratios yields an uncertainty in the oxygen abundance up to a factor of 5. Thus, calculating a meaningful normative mineralogy for Eros based on the present data set appears impossible.

Finally, it is worth noting an additional weakness in our data that appears insurmountable in the context of calculating a normative mineralogy. One of the earliest assignments made in a normative calculation is partitioning of  $SiO_2$  and  $Al_2O_3$  with CaO,  $Na_2O$  and  $K_2O$ . As  $SiO_2$  is partitioned with  $Na_2O$  and  $K_2O$  at a ratio of 3:1, the  $SiO_2$  abundance is particularly sensitive to the abundances of sodium and potassium. Further, the  $SiO_2$  abundance is critical in ultimately determining the orthopyroxene (hypersthene) to olivine ratio. However, we cannot measure the Na abundance (either absolute or elemental ratio) with either orbital x-ray or gamma-ray spectroscopy. Thus, even a near-perfect determination of major element abundances would still be of limited use in ultimately calculating the  $ol/(ol + px)$  ratio, and comparing that to values derived from spectra, without determining the sodium abundance.

### Matrix Inversion

A simultaneous solution for mineral abundances using known bulk and mineral compositions could provide an

independent test of the spectrally-derived olivine/pyroxene and orthopyroxene/clinopyroxene ratios. To this end, we have used a matrix inversion method to simultaneously solve for mineral abundance. A detailed example of this technique is given in Appendix B. Briefly, the method depends on the fact that the elemental abundance for any element ( $X$ ) is expressed as:

$$\text{Abundance } X = \sum \text{Abundance}_{\text{Mineral}} \times \text{Abundance}_{X \text{ in Mineral}}$$

For the NEAR data, we solved a series of matrices constrained by the bulk abundances of Fe, Mg, Si, Al, S and Ca and the mineral compositions of olivine, orthopyroxene, clinopyroxene, metal, sulfide and feldspar. As in the case of the normative mineralogy calculations, we assumed an Al abundance of 1.2% (appropriate to and invariant between H, L and LL ordinary chondrites; Nittler *et al.*, 2001), solved for Si using the average Al/Si ratio from the x-ray experiment, solved for S and Ca using the derived Si value and the S/Si and Ca/Si ratios from the x-ray experiment, and solved for Fe/Si and Mg/Si values using the ratios from either x-ray or gamma-ray experiments.

Mineral compositions were constrained by orthopyroxene compositions of Fs<sub>15</sub> and Fs<sub>25</sub> (bracketing that of ordinary chondrites; Gomes and Keil, 1980), a clinopyroxene composition of Fs<sub>10</sub>Wo<sub>45</sub> (McFadden *et al.*, 2001) and a Fa/Fs ratio of 1.18 (Gomes and Keil, 1980). Metal was assumed to be 100% iron. Sulfide was assumed to be stoichiometric FeS. An ordinary chondrite plagioclase composition was used.

Possible solutions were bracketed by calculating a range of solutions using x-ray and gamma-ray Fe/Si and Mg/Si ratios

and orthopyroxene compositions of Fs<sub>15</sub> and Fs<sub>25</sub>. The solutions are given in Table 3. A few features are noteworthy. Solutions to the matrices using the gamma-ray derived Fe/Si ratios give unreasonably low mineral abundances and, in the case of the Fs<sub>15</sub> orthopyroxene composition, unreasonably low olivine/pyroxene ratios. These low totals result from the low total abundance of Fe and moderately high abundance of Mg (relative to ordinary chondrites), which appears to favor the lower-FeO orthopyroxene preferentially over olivine. Without an imposed constraint on the olivine/pyroxene ratio, such as in the normalized element distribution method, the matrix inversion fails to yield a reasonable solution for the gamma-ray derived compositions.

The solutions to the matrices using the x-ray-derived compositions appear to yield more reasonable results. Mineral abundance totals are close to 100%. These results can be compared to ordinary chondrite abundances for H, L and LL chondrites, as well as to results from other methods. In using a Fs<sub>25</sub> orthopyroxene composition, appropriate to LL chondrites, we note that the calculated mineralogy has a higher olivine/pyroxene ratio and metal abundance and much lower orthopyroxene/clinopyroxene ratio than observed in LL chondrites. These results are consistent with the normalized element distribution results, which indicated a higher metal abundance. The solution constrained by a Fs<sub>15</sub> orthopyroxene composition, similar to H chondrites, contains roughly an H chondrite-like abundance of metal and olivine/pyroxene ratio, but a small overabundance of clinopyroxene. While this may reflect exclusion of some minerals actually observed in meteorites (*e.g.*, calcium phosphates) from our calculations,

TABLE 3. Derived mineralogies using matrix inversion for a range of orthopyroxene compositions and Mg/Si and Fe/Si ratios.

		H§		L§		LL§		
Opx Comp.	Assumed*	Fs <sub>25</sub> Wo <sub>0</sub>	Fs <sub>25</sub> Wo <sub>0</sub>	Fs <sub>15</sub> Wo <sub>0</sub>	Fs <sub>15</sub> Wo <sub>0</sub>	Fs <sub>17.2</sub>	Fs <sub>21.3</sub>	Fs <sub>24.1</sub>
Ol Comp.	Assumed†	Fa <sub>30</sub>	Fa <sub>30</sub>	Fa <sub>18</sub>	Fa <sub>18</sub>	Fa <sub>18.8</sub>	Fa <sub>24.6</sub>	Fa <sub>28.5</sub>
Cpx Comp.	Assumed*	Fs <sub>10</sub> Wo <sub>45</sub>	Fs <sub>10</sub> Wo <sub>45</sub>	Fs <sub>10</sub> Wo <sub>45</sub>	Fs <sub>10</sub> Wo <sub>45</sub>	—	—	—
Mg/Si	XRS-GRS‡	0.85	0.75	0.85	0.75	0.8	0.8	0.8
Fe/Si	XRS-GRS‡	1.65	0.8	1.65	0.8	1.0	1.2	1.6
Olivine	Calculated	61.3	43.2	39.7	24.9	35.0	44.8	51.9
Opx	Calculated	7.3	19.6	19.8	30.3	26.2	24.2	21.4
Cpx	Calculated	7.1	7.1	7.1	7.1	4.1	5	5.3
Plag	Calculated	10.5	10.5	10.5	10.5	9.6	10.3	10.3
Metal	Calculated	14.5	1.7	21.5	7.6	18.0	8.4	3.6
Sulfide	Calculated	0.7	0.7	0.7	0.7	5.5	5.8	5.9
Total	Calculated	101.4	82.8	99.3	81.1	98.4	98.5	98.4
%Ol	Calculated	81.0	61.8	59.6	40.0	53.6	60.5	66.0
%Opx/Px	Calculated	50.7	73.4	73.6	81.0	86.5	82.9	80.1

\*Assumed compositions of orthopyroxene and clinopyroxene appropriate to ordinary chondrites (Gomes and Keil, 1980; McFadden *et al.*, 2001).

†Assumed using a Fa/Fs ratio of 1.18 appropriate to equilibrated ordinary chondrites (Gomes and Keil, 1980).

‡Values derived from the XRS and GRS measurements (Nittler *et al.*, 2001; Evans *et al.*, 2001).

§Average normative mineralogies (McSween *et al.*, 1991) and mineral compositions (Gomes and Keil, 1980) for H, L and LL chondrites.



the results are consistent with the findings of McFadden *et al.* (2001), that suggested that matching the spectral parameters with an H-chondrite composition required an overabundance of clinopyroxene and, perhaps, a small degree of partial melting.

It should not be surprising that the matrix inversion yields results consistent with ordinary chondrites using input parameters (x-ray-derived composition, mineral compositions) consistent with ordinary chondrites. Changing a single input parameter (*e.g.*, changing the Al abundance to values appropriate to enstatite (~0.8 wt%) or carbonaceous (~1.5 wt%) chondrites) would not produce results consistent with different assemblages, since other factors (*e.g.*, mineral composition, elemental ratios) are also important influences and are considerably more constrained by XGRS and MSI/NIS data. Although the matrix results are broadly consistent with other lines of evidence, they point to ongoing inconsistencies between the various data sets. We do not believe that this method can easily constrain one model composition relative to another.

## CONCLUSIONS

Synthesizing data from the x-ray/gamma-ray spectrometers and near-infrared spectrometer/multi-spectral imager experiments from the NEAR mission points to some apparent inconsistencies in associating the composition of Eros with a single meteoritic analog. If constraints from each experiment are assumed to be indicative of the underlying bedrock of 433 Eros and a unique solution is sought, no meteoritic analog can be identified. This largely results from the combination of (1) near-chondritic x-ray-derived Mg/Si, Fe/Si, Al/Si and Ca/Si similar to H chondrites, (2) marked depletions, relative to ordinary chondrite in x-ray-derived S/Si, (3) marked depletions, relative to ordinary chondrites, of gamma-ray derived Fe/O and Fe/Si relative to all ordinary chondrites and the x-ray-derived ratios, (4) band II position most consistent with an orthopyroxene/clinopyroxene mixture similar to LL chondrites, and (5) derived olivine/pyroxene ratios which range between values appropriate to H chondrites and those of LL chondrites. These conflicting data sets, notably the differences in inferred mineral proportions and chemical ratios (*e.g.*, Fe/Si), cause us to question the basic assumption that the regolith of Eros is indicative of the composition of the underlying bedrock.

We have applied a variety of techniques to combine and synthesize these data sets. We believe that one cannot unequivocally determine a "best" meteoritic analog for 433 Eros when all of the data are considered. The most likely analogs are ordinary chondrites, which would require alteration at the surface by a range of processes to produce the S depletion, variable Fe/Si ratios and the spectral dissimilarity between Eros and laboratory spectra of ordinary chondrites. Also possible is a primitive achondrite analog derived from a precursor assemblage of the same mineralogy as the ordinary chondrite

groups, although the homogeneity of 433 Eros is more difficult to explain. The x-ray and gamma-ray compositions might be resolved by incorporation of different amounts of metal between the upper tens of centimeters analyzed by the gamma-ray spectrometer and the upper 100  $\mu\text{m}$  analyzed by the x-ray spectrometer. Metal ( $\pm$ sulfide) separation from silicates might occur either through physical migration (*e.g.*, the reverse Brazil Nut Effect or electrostatic levitation; Hong *et al.*, 2001; Robinson *et al.*, 2001) or partial melting (*e.g.*, McCoy *et al.*, 2000). It is more difficult to reconcile the apparent discrepancy between the preferred spectral analog (LL chondrites) and the preferred x-ray composition (H chondrites), though this might reflect systematic errors in deriving the Fe/Si ratio from the x-ray experiment (Nittler *et al.*, 2001).

While the NEAR mission to 433 Eros has greatly increased our understanding of this asteroid and the processes altering its surface, the inability to point to a single, unambiguous meteoritic analog is somewhat unsatisfying. Uncertainties stem from a number of factors. To confidently assert a single meteoritic analog, compositions (both mineralogical and chemical) must be determined with a degree of uncertainty less than the difference between the various groups. This is probably not possible for L vs. LL chondrites, but may be for H vs. L/LL chondrites. In the case of NEAR, solar monitors were less than optimal (Nittler *et al.*, 2001). This alone introduced considerable uncertainty and solar monitor design could certainly be improved for future missions. In addition, these missions could employ different instrument designs (*e.g.*, solid-state Si detectors in the x-ray system to reduce background) to decrease uncertainties.

The biggest obstacle, however, in identifying a meteoritic analog seems to be the lack of detailed understanding about the nature of chemical and physical processes (particularly volatilization, mineral migration and agglutinate formation) occurring in the regolith of asteroids. It is clear that meteoritic regolith breccias provide an imperfect record of modern asteroidal regolith (McKay *et al.*, 1989). Resolution of these issues for the Moon required both a detailed understanding of the distribution and gross structure of the regolith (McKay *et al.*, 1991) and submicron scale examination of individual grains from lunar regolith (Pieters *et al.*, 2000). A similar two-pronged attack for asteroids would seem warranted, with a rover that could examine the mineralogy, mineral abundances and textures at a meter- to centimeter-scale and sample return for characterization of regolith and bedrock. While MUSES-C will provide sample return, the unfortunate deletion of a rover from the mission will substantially reduce our understanding of the structure of the regolith.

*Acknowledgements*—The authors would like to thank NASA for its sponsorship of NEAR, the entire navigation team for making the science from this mission possible and Andy Cheng for his support of our efforts. Reviews by T. Swindle and C. Pieters helped clarify the manuscript.

*Editorial handling:* D. W. G. Sears

## REFERENCES

- BURBINE T. H., MCCOY T. J. AND BINZEL R. P. (2001a) Spectra of angrites and possible parent bodies (abstract). *Lunar Planet. Sci.* **32**, #1857, Lunar and Planetary Institute, Houston, Texas, USA (CD-ROM).
- BURBINE T. H., MCCOY T. J., NITTLER L. R. AND BELL J. F., III (2001b) Could 433 Eros have a primitive achondritic composition? (abstract). *Lunar Planet. Sci.* **32**, #1860, Lunar and Planetary Institute, Houston, Texas, USA (CD-ROM).
- CLARK B. E. *ET AL.* (2001) Space weathering on Eros: Constraints from albedo and spectral measurements of Psyche crater. *Meteorit. Planet. Sci.* **36**, 1617–1637.
- CLARKE R. S., JR., JAROSEWICH E., MASON B., NELEN J., GÓMEZ M. AND HYDE J. R. (1970) The Allende, Mexico, meteorite shower. *Smithson. Contrib. Earth Sci.* **5**, 1–53.
- CLOUTIS E., GAFFEY M. J., JACKOWSKI T. L. AND REED K. L. (1986) Calibration of phase abundance, composition, and particle size distribution for olivine-orthopyroxene mixtures from reflectance spectra. *J. Geophys. Res.* **91**, 11 641–11 653.
- COX K. G., BELL J. D. AND PANKHURST R. J. (1979) *The Interpretation of Igneous Rocks*. Allen and Unwin, St. Leonards, Australia. 450 pp.
- EATON N., GREEN S. F., MCCHEYENE R. S., MEADOWS A. J. AND VEEDER G. J. (1983) Observations of asteroids in the 3- to 4-micron region. *Icarus* **55**, 245–249.
- EVANS L. G., STARR R., BRÜCKNER J., REEDY R. C., BOYNTON W. V., TROMBKA J. I., GOLDSTEN J. O. AND MASARIK J. (2001) Elemental composition from gamma-ray spectroscopy of the *NEAR-Shoemaker* spacecraft's landing site on 433 Eros. *Meteorit. Planet. Sci.* **36**, 1639–1660.
- GAFFEY M. J. (1976) Spectral reflectance characteristics of the meteorite classes. *J. Geophys. Res.* **81**, 905–920.
- GAFFEY M. J., BELL J. F., BROWN R. H., BURBINE T. H., PIATEK J. L., REED K. L. AND CHAKY D. A. (1993) Mineralogical variations within the S-type asteroid class. *Icarus* **106**, 573–602.
- GASTINEAU H. K. AND MCSWEEN H. Y., JR. (2000) Oxidation during metamorphism of ordinary chondrites and implications for the NEAR mission to 433 Eros (abstract). *Lunar Planet. Sci.* **31**, #1406, Lunar and Planetary Institute, Houston, Texas, USA (CD-ROM).
- GOLDSTEN J. O. (1998) The NEAR X-ray/gamma-ray spectrometer. *Johns Hopkins APL Tech. Digest* **19**, 126–135.
- GOLDSTEN J. O. *ET AL.* (1997) The x-ray/gamma-ray spectrometer on the Near Earth Asteroid Rendezvous mission. *Space Sci. Rev.* **82**, 169–216.
- GOMES C. B. AND KEIL K. (1980) *Brazilian Stone Meteorites*. Univ. New Mexico Press, Albuquerque, New Mexico, USA. 162 pp.
- HAWKINS S. E., III (1998) The NEAR multispectral imager. *Johns Hopkins APL Tech. Digest* **19**, 107–114.
- HAWKINS S. E., III *ET AL.* (1997) Multi-spectral imager on the Near Earth Asteroid Rendezvous mission. *Space Sci. Rev.* **82**, 31–100.
- HONG D. C., QUINN P. V. AND LUDING S. (2001) The Reverse Brazil Nut Problem: Competition between percolation and condensation. *Phys. Rev. Lett.* **86**, 3423–3426.
- KEIL K. (1989) Enstatite meteorites and their parent bodies. *Meteoritics* **24**, 195–208.
- LUCEY P. G., HINRICHS J. L., URQUHART-KELLY M., WELLNITZ D., BELL J. F., III AND CLARK B. E. (2001) Thermo-reflectance spectra of Eros: Unambiguous detection of olivine (abstract). *Lunar Planet. Sci.* **32**, #1490, Lunar and Planetary Institute, Houston, Texas, USA (CD-ROM).
- MCCOY T. J., NITTLER L. R., BURBINE T. H., TROMBKA J. I., CLARK P. E. AND MURPHY M. E. (2000) Anatomy of a partially-differentiated asteroid: A "NEAR"-sighted view of acapulcoites and lodranites. *Icarus* **148**, 29–36.
- MCKAY D. S., SWINDLE T. D. AND GREENBERG R. (1989) Asteroidal regoliths: What we do not know. In *Asteroids II* (eds. R. P. Binzel, T. Gehrels and M. S. Matthews), pp. 617–642. Univ. Arizona Press, Tucson, Arizona, USA.
- MCKAY D. S., HEIKEN G., BASU A., BLANFORD G., SIMON S., REEDY R., FRENCH B. M. AND PAPIKE J. (1991) The lunar regolith. In *Lunar Sourcebook* (eds. G. H. Heiken, D. T. Vaniman and B. M. French), pp. 285–356. Cambridge Univ. Press, New York, New York, USA.
- MCFADDEN L. A., WELLNITZ D. D., SCHNAUBELT M., GAFFEY M. J., BELL J. F., III, CLARK B. E., IZENBERG N., MURCHIE S., CHAPMAN C. R. AND LUCEY P. G. (2001) Mineralogical interpretation of reflectance spectra from NEAR NIS low phase flyby. *Meteorit. Planet. Sci.* **36**, 1711–1726.
- MCSWEEN H. Y., JR., BENNETT M. E., III AND JAROSEWICH E. (1991) The mineralogy of ordinary chondrites and implications for asteroid spectrophotometry. *Icarus* **90**, 107–116.
- MCSWEEN H. Y., JR. *ET AL.* (1999) Chemical, multispectral, and textural constraints on the composition and origin of rocks at the Mars Pathfinder landing site. *J. Geophys. Res.* **104**, 8679–8715.
- MITTFELDELT D. W., MCCOY T. J., GOODRICH C. A. AND KRACHER A. (1998) Non-chondritic meteorites from asteroidal bodies. In *Planetary Materials* (ed. J. J. Papike), pp. 4-1 to 4-195. *Rev. Mineral* **36**, Mineral. Soc. Amer., Washington, D.C., USA.
- MURCHIE S. L. AND PIETERS C. M. (1996) Spectral properties and rotational spectral heterogeneity of 433 Eros. *J. Geophys. Res.* **101**, 2201–2214.
- NITTLER L. R. *ET AL.* (2001) X-ray fluorescence measurements of the surface elemental composition of asteroid 433 Eros. *Meteorit. Planet. Sci.* **36**, 1673–1695.
- PEACOCK K., WARREN J. W. AND DARLINGTON E. H. (1998) The near-infrared spectrometer. *Johns Hopkins APL Tech. Digest* **19**, 115–125.
- PIETERS C. M., TAYLOR L. A., NOBLE S. K., KELLER L. P., HAPKE B., MORRIS R. V., ALLEN C. C., MCKAY D. S. AND WENTWORTH S. (2000) Space weathering on airless bodies: Resolving a mystery with lunar samples. *Meteorit. Planet. Sci.* **35**, 1101–1107.
- ROBINSON M. S., THOMAS P. C., VEVERKA J. AND MURCHIE S. (2001) 433 Eros regolith: Implications for global stratigraphy, sedimentary processes, and degradation rates (abstract). *Meteorit. Planet. Sci.* **36 (Suppl.)**, A174–A175.
- TROMBKA J. I. *ET AL.* (1997) Compositional mapping with the NEAR X-ray/gamma-ray spectrometer. *J. Geophys. Res.* **102**, 23 729–23 750.
- VEVERKA J. *ET AL.* (2000) NEAR at Eros: Imaging and spectral results. *Science* **289**, 2088–2097.
- VEVERKA J. *ET AL.* (2001) The landing of the NEAR-Shoemaker spacecraft on asteroid 433 Eros. *Nature* **413**, 390–393.
- WARREN J. W., PEACOCK K., DARLINGTON E. H., MURCHIE S. L., ODEN S. F., HAYES J. R., BELL J. F., III, KREIN S. J. AND MASTANDREA A. (1997) Near infrared spectrometer for the Near Earth Asteroid Rendezvous mission. *Space Sci. Rev.* **82**, 101–167.
- WETHERILL G. W. AND CHAPMAN C. R. (1988) Asteroids and meteorites. In *Meteorites and the Early Solar System* (eds. J. F. Kerridge and M. S. Matthews), pp. 35–67. Univ. Arizona Press, Tucson, Arizona, USA.

## APPENDIX A

Sample calculation for normalized element distribution calculation  $\text{Fs}_{15}\text{Wo}_0$ , olivine/pyroxene ratio of 58:42 and using the bulk assuming a two-pyroxene system, orthopyroxene composition of composition determined by the XRS experiment (Nittler *et al.*, 2001).

- (1) Partition iron between metal, sulfide and silicate using  $\text{Fe}_{\text{metal}}/\text{Si} = \text{Fe}_{\text{total}}/\text{Si} - \text{Fe}_{\text{sulfide}}/\text{Si} - \text{Fe}_{\text{silicate}}/\text{Si}$
- |                                      |      |                              |
|--------------------------------------|------|------------------------------|
| $\text{Fe}_{\text{total}}/\text{Si}$ | 1.65 | Eros global average from XRS |
|--------------------------------------|------|------------------------------|
- (1a) Calculate  $\text{Fe}_{\text{sulfide}}/\text{Si}$  assuming an Fe/S ratio and using the measured S/Si ratio
- |  |       |   |
|--|-------|---|
| $\text{Fe}_{\text{sulfide}}/\text{Si}$ | 0.024 | = $\text{Fe}/\text{S} \times \text{S}/\text{Si}$        |
| Fe/S                                   | 1.74  | Mass ratio appropriate to stoichiometric FeS (troilite) |
| S/Si                                   | 0.014 | Eros global average from XRS                            |
- (1b) Calculate the  $\text{Fe}_{\text{silicate}}/\text{Si}$  ratio by first calculating the %mafics/silicates and multiply by the Fe/Si ratio of the mafics
- |  |       |  |
|--|-------|--|
| $\text{Fe}_{\text{silicates}}/\text{Si}$ | 0.421 | = %mafics silicate/total silicates $\times$ Fe/Si (mafics silicates)   |
| (Fe/Si) <sub>opx</sub>                   | 0.30  | Fe/Si ratio for $\text{Fs}_{15}\text{Wo}_0$ (low-FeO range of ordinary chondrites)   |
| (Mg/Si) <sub>opx</sub>                   | 0.65  | Mg/Si ratio for $\text{Fs}_{15}\text{Wo}_0$  |
| (Fe/Si) <sub>cpx</sub>                   | 0.20  | Fe/Si ratio for $\text{Fs}_{10}\text{Wo}_{45}$ (clinopyroxene component for two-pyroxene mixing model of McFadden <i>et al.</i> , 2001)  |
| (Mg/Si) <sub>cpx</sub>                   | 0.39  | Mg/Si ratio for $\text{Fs}_{10}\text{Wo}_{45}$   |
| (Fe/Si) <sub>ol</sub>                    | 0.72  | Fe/Si ratio for $\text{Fa}_{18}$ (olivine composition using Fa/Fs ratio of 1.18 appropriate for co-existing silicates in equilibrium; Gomes and Keil, 1980)  |
| (Mg/Si) <sub>ol</sub>                    | 1.42  | Mg/Si ratio for $\text{Fa}_{18}$   |
| (Mg/Si) <sub>mafics</sub>                | 1.07  | = $((\text{Mg}/\text{Si})_{\text{ol}} \times 0.58) + ((\text{Mg}/\text{Si})_{\text{opx}} \times 0.42 \times 0.76) + ((\text{Mg}/\text{Si})_{\text{cpx}} \times 0.42 \times 0.24)$<br>appropriate for an ol/px ratio of 58:42 and an opx/cpx ratio of 76:24 |
| (Mg/Si) <sub>XRS</sub>                   | 0.85  | Eros global average from XRS   |
| Mafics/Silicates                         | 0.795 | = $(\text{Mg}/\text{Si})_{\text{XRS}}/(\text{Mg}/\text{Si})_{\text{mafics}}$   |
| (Fe/Si) <sub>mafics</sub>                | 0.53  | Same formula as $(\text{Mg}/\text{Si})_{\text{mafics}}$ adapted for Fe/Si  |
| $\text{Fe}_{\text{metal}}/\text{Si}$     | 1.204 | = $\text{Fe}_{\text{total}}/\text{Si} - \text{Fe}_{\text{sulfide}}/\text{Si} - \text{Fe}_{\text{silicate}}/\text{Si}$  |
- (2) Calculate the %plag/silicate by assuming an Al/Si ratio for plag and using the measured Al/Si ratio
- |                         |       |  |
|-------------------------|-------|--|
| (Al/Si) <sub>plag</sub> | 0.378 | Appropriate to a chondritic composition of $\text{An}_{12.6}\text{Or}_{3.8}$ |
| (Al/Si) <sub>XRS</sub>  | 0.068 | Eros global average from XRS   |
| Plag/silicates          | 0.180 | = $(\text{Al}/\text{Si})_{\text{XRS}}/(\text{Al}/\text{Si})_{\text{plag}}$   |
- (3) Calculate the Si/Silicates ratio to convert mineral/Si ratios to mineral/silicate
- |              |       |  |
|--------------|-------|--|
| Si/Silicates | 0.228 | = $\Sigma (\text{Si}/\text{oxide total})_{\text{Silicate } X} \times (\% \text{Silicate } X / \text{Total silicates})$ |
|--------------|-------|--|
- (4) Calculate the mineral/silicate ratios
- |                   |       |  |
|-------------------|-------|--|
| Mafics/Silicates  | 0.795 |  |
| Plag/Silicates    | 0.180 |  |
| Metal/Silicates   | 0.274 | = $\text{Fe}_{\text{metal}}/\text{Si} \times \text{Si}/\text{Silicates}$   |
| Sulfide/Silicates | 0.009 | = $\text{Fe}_{\text{sulfide}}/\text{Si} \times \text{Si}/\text{Silicates} \times \text{mol. wt. FeS}/\text{mol. wt. Fe}$ |
- (5) Normalize all minerals to 100%
- |           |      |  |
|-----------|------|--|
| Silicates | 78.0 | = $100 \div (1 + (\text{Metal}/\text{Silicates}) + (\text{Sulfide}/\text{Silicates}))$ |
| Metal     | 21.4 | = Silicates $\times$ Metal/Silicates   |
| Sulfides  | 0.68 | = Silicates $\times$ Sulfides/Silicates  |
- (6) Distribute total silicate between olivine, orthopyroxene, clinopyroxene and plagioclase
- |               |      |  |
|---------------|------|--|
| Olivine       | 36.0 | = Silicates $\times \text{Ol}/(\text{Ol} + \text{Px}) \times \text{Mafics}/\text{Silicates}$   |
| Orthopyroxene | 19.8 | = Silicates $\times \text{Px}/(\text{Ol} + \text{Px}) \times \text{Opx}/(\text{Opx} + \text{Cpx}) \times \text{Mafics}/\text{Silicates}$ |
| Clinopyroxene | 6.3  | = Silicates $\times \text{Px}/(\text{Ol} + \text{Px}) \times \text{Cpx}/(\text{Cpx} + \text{Opx}) \times \text{Mafics}/\text{Silicates}$ |
| Plagioclase   | 14.0 | = Silicates $\times \text{Plag}/\text{Silicates}$  |
| Metal         | 21.4 | = Metal  |
| Sulfide       | 0.7  | = Sulfides   |

## APPENDIX B

Sample calculation for a simultaneous solution using matrix inversion calculation assuming a two-pyroxene system, orthopyroxene composition of  $Fs_{15}Wo_0$  and using the bulk composition determined by the XRS experiment (Nittler *et al.*, 2001).

(1) Express each element as  $\Sigma \text{Abundance}_{\text{Mineral}} \times \text{Abundance}_{X \text{ in Mineral}}$ .

$$\text{Fe} = \text{Ol} \times \text{Fe}_{\text{ol}} + \text{Opx} \times \text{Fe}_{\text{opx}} + \text{Cpx} \times \text{Fe}_{\text{cpx}} + \text{Metal} \times \text{Fe}_{\text{metal}} + \text{Sulfide} \times \text{Fe}_{\text{sul}} + \text{Feld} \times \text{Fe}_{\text{feld}}$$

$$\text{Mg} = \text{Ol} \times \text{Mg}_{\text{ol}} + \text{Opx} \times \text{Mg}_{\text{opx}} + \text{Cpx} \times \text{Mg}_{\text{cpx}} + \text{Metal} \times \text{Mg}_{\text{metal}} + \text{Sulfide} \times \text{Mg}_{\text{sul}} + \text{Feld} \times \text{Mg}_{\text{feld}}$$

$$\text{Si} = \text{Ol} \times \text{Si}_{\text{ol}} + \text{Opx} \times \text{Si}_{\text{opx}} + \text{Cpx} \times \text{Si}_{\text{cpx}} + \text{Metal} \times \text{Si}_{\text{metal}} + \text{Sulfide} \times \text{Si}_{\text{sul}} + \text{Feld} \times \text{Si}_{\text{feld}}$$

$$\text{Al} = \text{Ol} \times \text{Al}_{\text{ol}} + \text{Opx} \times \text{Al}_{\text{opx}} + \text{Cpx} \times \text{Al}_{\text{cpx}} + \text{Metal} \times \text{Al}_{\text{metal}} + \text{Sulfide} \times \text{Al}_{\text{sul}} + \text{Feld} \times \text{Al}_{\text{feld}}$$

$$\text{S} = \text{Ol} \times \text{S}_{\text{ol}} + \text{Opx} \times \text{S}_{\text{opx}} + \text{Cpx} \times \text{S}_{\text{cpx}} + \text{Metal} \times \text{S}_{\text{metal}} + \text{Sulfide} \times \text{S}_{\text{sul}} + \text{Feld} \times \text{S}_{\text{feld}}$$

$$\text{Ca} = \text{Ol} \times \text{Ca}_{\text{ol}} + \text{Opx} \times \text{Ca}_{\text{opx}} + \text{Cpx} \times \text{Ca}_{\text{cpx}} + \text{Metal} \times \text{Ca}_{\text{metal}} + \text{Sulfide} \times \text{Ca}_{\text{sul}} + \text{Feld} \times \text{Ca}_{\text{feld}}$$

(2) Rearrange into matrix form.

Fe	=	Ol	×	Fe <sub>ol</sub>	Fe <sub>opx</sub>	Fe <sub>cpx</sub>	Fe <sub>metal</sub>	Fe <sub>sul</sub>	Fe <sub>feld</sub>
Mg		Opx		Mg <sub>ol</sub>	Mg <sub>opx</sub>	Mg <sub>cpx</sub>	Mg <sub>metal</sub>	Mg <sub>sul</sub>	Mg <sub>feld</sub>
Si		Cpx		Si <sub>ol</sub>	Si <sub>opx</sub>	Si <sub>cpx</sub>	Si <sub>metal</sub>	Si <sub>sul</sub>	Si <sub>feld</sub>
Al		Metal		Al <sub>ol</sub>	Al <sub>opx</sub>	Al <sub>cpx</sub>	Al <sub>metal</sub>	Al <sub>sul</sub>	Al <sub>feld</sub>
S		Sulfide		S <sub>ol</sub>	S <sub>opx</sub>	S <sub>cpx</sub>	S <sub>metal</sub>	S <sub>sul</sub>	S <sub>feld</sub>
Ca		Feldspar		Ca <sub>ol</sub>	Ca <sub>opx</sub>	Ca <sub>cpx</sub>	Ca <sub>metal</sub>	Ca <sub>sul</sub>	Ca <sub>feld</sub>

(3) Substitute values (see text for explanation).

29.12	=	Ol	×	13.14	8.08	5.07	100	63.53	0
15.00		Opx		26.05	19.96	9.95	0	0	0
17.65		Cpx		18.70	26.41	25.80	0	0	30.29
1.20		Metal		0	0	0	0	0	11.48
0.25		Sulfide		0	0	0	0	36.47	0
1.36		Feldspar		0	0	16.42	0	0	1.87

(4) Matrix inversion yields the following mineral abundances (wt%).

Olivine	39.7
Orthopyroxene	19.8
Clinopyroxene	7.1
Plagioclase	10.5
Metal	21.5
Sulfide	0.7